INTERNATIONAL SOCIETY FOR SOIL MECHANICS AND GEOTECHNICAL ENGINEERING

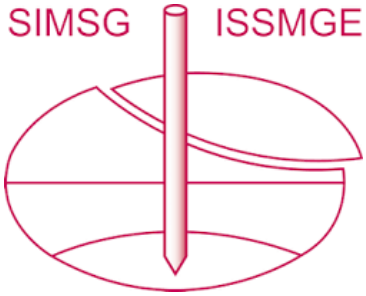

This paper was downloaded from the Online Library of the International Society for Soil Mechanics and Geotechnical Engineering (ISSMGE). The library is available here:

https://www.issmge.org/publications/online-library

This is an open-access database that archives thousands of papers published under the Auspices of the ISSMGE and maintained by the Innovation and Development Committee of ISSMGE.

The paper was published in the proceedings of the 20th International Conference on Soil Mechanics and Geotechnical Engineering and was edited by Mizanur Rahman and Mark Jaksa. The conference was held from May 1st to May 5th 2022 in Sydney, Australia.

Proceedings of the 20th International Conference on Soil Mechanics and Geotechnical Engineering– Rahman and Jaksa (Eds)
© 2022 Australian Geomechanics Society, Sydney, Australia, ISBN 978-0-9946261-4-1

Numerical computer modelling of a sustainable road structure with geogrids in a karst hazard environment

Modélisation numérique par ordinateur d'une structure routière durable à l'aide de géogrilles dans un environnement à risque karstique

Alain L. Conrado-Palafox
University of Western Ontario, Ontario, Canada, aconrado@uwo.ca

Luisa N. Equihua-Anguiano
GEIC-CFE Comisión Federal de Electricidad, San Juan, Ciudad de México, México

ABSTRACT: Design of the road infrastructure must be sustainability for any geotechnical challenge caused for the different natural hazards. In the case of the karst terrains, the material dissolution develops many cavities in the ground that finishing generally in a surface subsidence or in the soil failure. In this way, a solution is to add geogrids in a road structure to mitigate the road failure. This paper presents a numerical study of the geogrid addition behavior in the road structure considering the effects of the cavities in the soil in a karst environment. The methodology to model cavities in Plaxis 2D ® was to model it as a tunnel, iterating the internal pressure until the minimum pressure to avoid collapse. Road structure was modelled in four steps in order to add geogrids between the four road layers, corresponding to the subgrade (divided in two thickness), base course and the asphalt concrete. Additionally, a static load was applied in the road surface. The results indicate that the best geogrid inclusion position is in the subgrade layer generating less tensile stress in the road structure because in that position the geogrids have an increase in their normal stiffness, improving the road structure despite cavities. Furthermore, it is presented the variation of the stresses in the road structure considering the best enhance with geogrids and without geogrids, to compare stress paths in the road structure. In conclusion, the geogrids are a satisfactory reinforcement for the road in a karst environment.

RÉSUMÉ : La conception de l'infrastructure routière doit être durable pour tout défi géotechnique posé par les différents risques naturels. Dans le cas des terrains karstiques, la dissolution des matériaux développe de nombreuses cavités dans le sol qui conduisent généralement à un affaissement de la surface ou à une rupture du sol. De cette façon, une solution pour atténuer l'effondrement de la route consiste à ajouter des géogrilles dans une structure routière. Cet article présente une étude numérique du comportement de l'ajout de géogrilles dans la structure routière en considérant les effets qu'ont les cavités dans le sol dans un environnement karstique. La méthodologie pour modéliser les cavités avec Plaxis 2D ® a été de le modéliser comme un tunnel, en itérant la pression interne jusqu'à la pression minimale afin d'éviter l'effondrement. La structure de la route a été modélisée en quatre étapes afin d'ajouter des géogrilles entre les quatre couches de la route, correspondant à la sous-couche (divisée en deux épaisseurs), à la couche de base et au béton bitumineux. De même, une charge statique a été appliquée dans la surface de la route. Les résultats indiquent que la meilleure position d'inclusion des géogrilles se trouve dans la couche de fondation, qui génère moins de contraintes de traction dans la structure de la route car, dans cette position, les géogrilles ont une augmentation de leur rigidité normale, ce qui améliore la structure de la route malgré les cavités. En outre, il est présenté la variation des contraintes dans la structure routière en considérant la meilleure amélioration avec les géogrilles et sans les géogrilles, pour comparer les chemins de contrainte dans la structure routière. En conclusion, l'ajout de géogrilles est un renforcement approprié pour la route dans un environnement karstique.

KEYWORDS: Computational mechanics; karst terrain; road & highways; geogrids; stress paths.

1 INTRODUCTION

Infrastructure developments such as roads, tunnels or bridges in karst geomorphology presents high risk of geological disasters such as rock collapse or surface subsidence (Xu, et al. 2018). To ensure the stability for different earth structures such as embankments, pavements and foundations, geogrids have been efficient as a reinforcement method (Hussein & Meguid 2016). For this reason, the present study focuses on the geogrid as a solution to prevent surface damage in the road structure due to several cavities presented in a karst terrain, specifically a typical road structure over a Mexican karst terrain.

Yucatan peninsula is in the southwest of Mexico. Its terrain is composed principally by limestones, dolomites and evaporate and for its geological conditions the water storage and the groundwater flow occur in the karstic zone (Bauer-Gottwein, et al. 2011). Yucatan has 3 primordial karst zones, the hill region, the central and the coast, all of them with different types of cavities from voids with 50cm of diameter to huge caves of 50m of diameter and some of them are flooded (Finch 1968). Figure 1a, illustrates an old embankment in Yucatan and Figure 1b illustrates a sinkhole next to the old embankment and Figure 1c show the cavity next to a highway.

The collapse of sinkholes in Yucatan is an inevitable consequence because the calcareous subsoil experiences excessive tensile stresses by the geo-material dissolution (Smart, et al 2006), therefore, this paper carried out a numerical FEM modeling to analyze the behavior of a road structure with geogrids in order to analyze the performance of the structure with and without geogrids when there are cavities in a specific area in the model.

2 MATERIALS AND METHOD

2.1 *Problem definition*

Study area was 200m long by 50m deep and typical stratigraphy of Yucatan with a 5.0m of a limestone bedrock thickness underlain by a granular soil with 45.0m of thickness (Estrada-

Media & Wes 2010). Additionally, the voids are developed between the bedrock and granular soil layers. A principal cavity was placed in the center of the model and the others 4 cavities were created in a symmetrical mode with the minimum internal pressure to avoid collapse of the cavity (Conrado-Palafox, et al. 2019). The diameters of the voids were 1m with a separation of 10m between them, additionally over the terrain a typical highway was imposed with a width of 8m (See Figure 2).

To obtain the stress paths of the road structure depending on the cavities and the position of the geogrids, a model composed of three principal phases was modelled (Table 1). The phase 1 represents the *in-situ* stresses due to the weight of the geo materials, a second phase was created with the road structure considering three different layers with the geogrids (road structure phase), subsequently, the heavy truck load (4.84kN/m2) is applied. In the last phase, cavities began to be generated in a symmetrical manner in the model, starting with one cavity in the middle and finishing with 5 cavities (two on each side). Finally, all cases were analyzed with an interface value of 0.67 (Rinter) (Oh 2011) to include the interaction between the geogrid and the road layers. It should be noted, the main goal of this study, is determining the response of the subgrade and base course layer due to the cavities in the model. For this reason, the truck load was modelled statically and in future investigations the cyclic load will be analyzed.

Figure 1. (a) An old embankment in Yucatan, (b) a sinkhole next to the old embankment and (c) a sinkhole next to the road at 1.5km from the previous sinkhole.

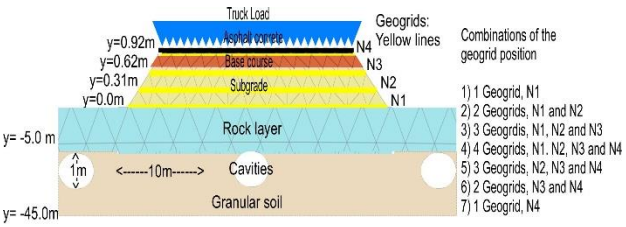

Figure 2. Finite element model with the road structure, the cavities, and the different combinations of the geogrids (N1, N2, N3 and N4) location.

Table 1. Phases in the numerical medialization.

Phases	*Condition*
Initial	Stratigraphy (rock layer and granular soil)
Road structure	Different road layers and the geogrids combinations as described in Figure 2
Static load	Truck load in the road surface (4.84kN/m^2)
Cavities	1 Cavity in the granular soil on central axis
	3 Cavities in the granular soil
	5 Cavities in the granular soil

2.2 *Geotechnical parameters*

"Hoek-Brown" Constitutive model was used to simulate the bedrock and the "Mohr-Coulomb" was used to model the second layer. Bedrock has an elastic behavior, and the soil is considered to have an elastic-perfectly behavior. Bedrock parameters were obtained from a core extraction to obtain the compressive uniaxial (σ_{ci}) of the intact rock, the earth pressure (k) is assumed as Eq. 1 (Sheorey 1994), besides, the rock mass was assumed with a Geological Strength Index (*GSI*) of 30 because the rock mass derives from unconsolidated marine residues (Lopez-Ramos 1975), which through the action of dissolution and compaction, it has resulted in a consolidated material with massive consistency, nevertheless with several joints. The granular soil parameters were obtained from Standard Penetration Test (*SPT*) and correlated with (VDOT 2013) to obtain effective parameters cohesion (*C'*) and friction angle (ϕ').

$$k = 0.25 + 7(E)(0.001 + 1/y) \quad (1)$$

where k is Earth Pressure (-), E is Elastic Modulus (*GPa*) and y is Vertical depth (m)

Additionally, typical values of geo material parameters from Yucatan for the road structure (subgrade, base course) were used to carry out this numerical model. The elastic modulus of the asphalt layer was selected according several finite element models such as Ahirwar & Mandal, 2017; Siriwardane et al, 2010, Faheem & Ahmed 2014. The polypropylene biaxial geogrid modeled in this investigation, is used to increase the stiffness of the road structure, and mitigate the soil failure, receiving the tension forces induced by the cavities in the model. Nowadays, it can be found geogrids with different axial stiffnesses 250, 525, 1025 kN/m (Jiang & Nimbalkar, 2019) and according Benmebarek et al, 2015, a geogrid with 580 kN/m modeled in Plaxis showed an adequate performance. In this investigation the axial stiffness selected was 250 kN/m being

the least resistance to analyze if there is an improvement. The detail of input parameters can be found in Table 2.

Table 2. FEM input parameters.

Layer / Parameters	*Value*	*Unit*
Asphalt concrete (Linear Elastic)		
Soil unit weight (γ)	23	kN/m^3
Elastic modulus (*E*)	2x10^6	kN/m^2
Poisson ratio (*v*)	0.25	-
Base course (Mohr-Coulomb)		
Soil unit weight (γ)	17	kN/m^3
Elastic modulus (*E*)	345,000	kN/m^2
Friction angle (ϕ)	40	◦
Poisson ratio (*v*)	0.35	-
Subgrade (Mohr-Coulomb)		
Soil unit weight (γ)	15	kN/m^3
Elastic modulus (*E*)	170,000	kN/m^2
Friction angle (ϕ)	34	◦
Poisson ratio (*v*)	0.4	-
Granular Soil (Mohr-Coulomb)		
Soil unit weight (γ)	10.1	kN/m^3
Elastic modulus (*E*)	20,000	kN/m^2
Friction angle (ϕ)	26	◦
Poisson ratio (*v*)	0.33	-
Bedrock (Hoek-Brown)		
Soil unit weight (γ)	12.2	kN/m^3
Elastic modulus (*E*)	2.55x10^6	kN/m^2
Friction angle (ϕ)	24.3	◦
Poisson ratio (*v*)	0.25	-
Geogrid (Normal Stiffness)		
Axial Stiffness (EA)	250	kN/m

2.3 *Stress paths*

The parameters of stresses, such as the desviator stress (Eq. 2) and the mean effective stress (Eq. 3), are widely used in geotechnics (Parry, 2004). The stress paths indicate the behavior of the initial and final stress of the material, for example, if the stresses start at any point of the *in-situ* stress (K_0) and then σ'$_1$ increases, the path will move to the area "A" (compression behavior with a horizontal deformation), nevertheless, if σ'$_3$ increases at the same time, the stress path will move to point "D" (compression behavior with a vertical extension). The stress paths are described in Figure 3, considering that σ'$_1$ is acting in the vertical plane.

$$q = (\sigma'_1 - \sigma'_3)/2 \quad (2)$$

$$p' = (\sigma'_1 + \sigma'_3)/2 \quad (3)$$

Where q = desviator stress (kN/m^2), p' = mean effective stress (kN/m^2), σ'_1 = major effective principal stress (kN/m^2) and σ'_3 = minor effective principal stress (kN/m^2).

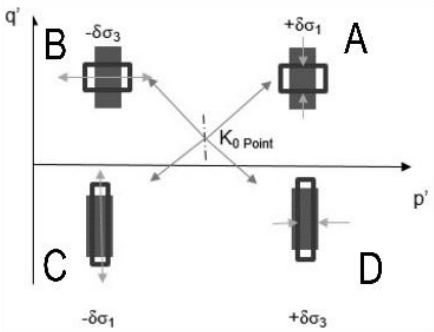

Figure 3. Stress Path considering the major effective principal stress (σ'1) acting in the vertical plane.

3 RESULTS

3.1 *Stress paths and Shear strain in the top of the subgrade layer*

Figure 4 shows the stress paths ($q - p'$) behavior in the middle top of the subgrade layer for the different combinations of the geogrid positions. To begin with, the black dot line represents the performance of the structure without geogrids and the first paths of the layer are in the compression zone when the structure and the load truck (blue square and orange diamond respectively) are applied. However, the cavities change the desviator stress in the layer because the σ'$_3$ increases (yellow triangle, green cross and red line marks) while the mean effective stress does vary.

Specifically, with the geogrid combination N2 (geogrids in y=0.0m and 0.31m), black dashed line in the Figure 4, the middle top of the subgrade layer generates less stresses in the structure than without geogrids, involving a less compression state. Furthermore, when the cavities are present, the reduction in the deviator stress is more noticeable, showing an extension state due to the increase of the horizontal stress (σ_3). As well as the geogrid combination N5 produced the same behavior (geogrids in y= 0.31m, 0.62m and 0.92m), grey continuous line in the Figure 4.

On the other hand, when the geogrids are embedded in the base course layer N6 (geogrids in y=0.62m and y=0.92m) or only placed in the foundation of the road structure (N1, geogrid in y=0.0m), black continuous line and grey dashed line respectively. The middle top of the subgrade layer generates less compression in the first two steps (road structure and static load), but when the cavities are in the model, the subgrade layer continues in the compression state, increasing its desviator and mean effective stresses.

Figure 5 shows the stress - strain ($q - \delta$) behavior in the middle top of the subgrade layer for the different combinations of the geogrid positions. When the road structure is imposed, the linear deformation is maintained in all the cases analyzed, with the main different that although the desviator stress decreases when the road structure has geogrids, the shear strain

is greater. This behavior is more notorious with the combination N1.

Subsequently and for all cases, when the truck load is imposed in the model the desviator increase for the vertical stress (σ_1) but the increase of the shear strain is less than the previous phase (road structure). However, the road structure without geogrids (black dot line) maintains its previous strain even with the cavities.

On the other hand, when there are geogrids in the road structure the performance is different depending on the position of the geogrids. For example, for the combination N2 and N5 the deviator stress decrease with the first cavity (yellow triangle mark) and the strain continues increasing. Nevertheless, with three and five cavities (green cross and red line marks respectively) the strain decreases because in these phases there are an increase in the horizontal stress causing a vertical deformation.

The previous performance is repeated for the combination N1 and N6, the desviator strain keeps increasing while the strain changes its direction in the last two cavity phases. Therefore, the reduction in the strain is due to the deformation created for the third and fifth cavity.

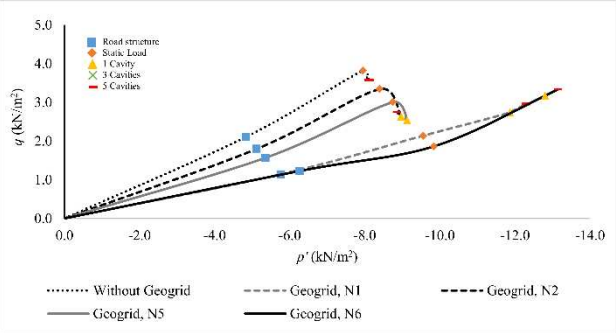

Figure 4. Stress paths measured at the middle top of the subgrade layer (y= 0.62m) for the different geogrid combinations.

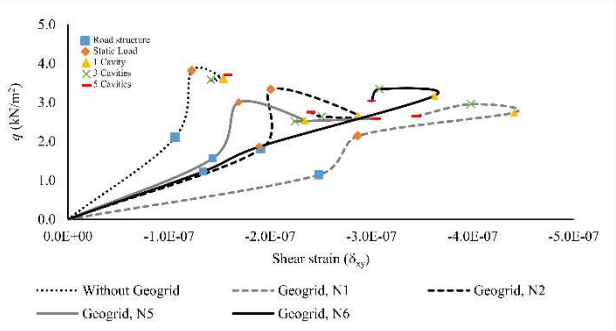

Figure 5. Desviator stress versus shear strain measured at the middle top of the base course layer (y= 0.62m) for the different geogrid combinations.

3.2 *Stress paths in the top of the base course layer*

Figure 6 shows the stress paths ($q - p'$) behavior in the middle top of the base course layer for the different combinations of the geogrid positions. To begin with, the structure without geogrids (the black dot line) has the same behavior as in the subgrade layer. With an importance performance, the combination N2 and N5 had less stresses than the combinations N1 and N6. Mainly because the N1 and N6 combinations continue increasing their stresses in the subgrade layer and the combinations N2 and N5 do not.

Certainly, the behavior of the base course is based on the compression due to the increase of the σ'_1, however, when the σ'_3 increased in the subgrade layer benefits to the base course layer to end with less stresses.

4 CONCLUSIONS

This study presents numerical FEM models to verify the effect of the road structure reinforcement provided by geogrids when there are cavities in the ground. A conceptual model with a realistic karst lithology from Yucatan, Mexico has been modelled. Furthermore, five cavities have been included in the terrain with the minimum internal pressure to avoid the collapse of the terrain. The results have been presented for stress paths and stress strains in the top of the subgrade and the base course layers. The main findings of this study include:

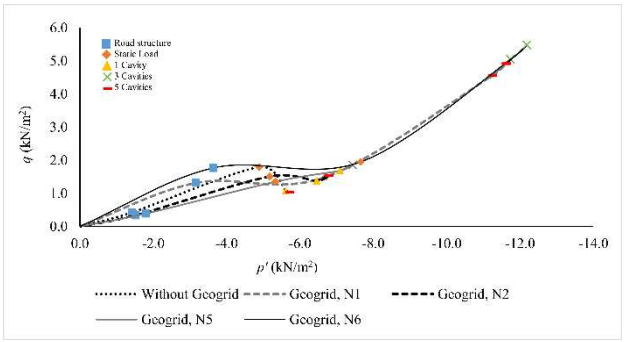

Figure 6. Stress paths measured at the middle top of the base course layer (y= 0.92m) for the different geogrid combinations.

- Subgrade layer
- The reduction of the compression state in the subgrade layer due to the geogrids in the different positions.
- The change of the stress paths due to the cavities, decreasing the desviator stress while the mean stress keeps the same value, for the geogrid combination N2 and N5.
- The stress paths for the combination N1 and N6 do not change its behavior with the cavities because the desviator and the main stresses continue increasing.
- The relaxation in the subgrade layer is visualized in the green cross mark when the shear strain changed its direction causing an extension in the layer.

- Base course layer
- The compression state behaviour in the base course layer due to the cavities in the ground.
- The reduction of the base course stresses with the combination N2 and N5 because the geogrids dissipated the stresses before reaching the base course layer.

Based on the results, the geogrid combination N2 has the better performance in both top layers the subgrade and the base course. It should be noted that additional studies are needed to improve the computational karstic model for example use a cyclic load in the crest of the road.

5 REFERENCES

Ahirwar, S.K., Mandal, J.N. 2017. Finite Element Analysis of Flexible Pavement with Geogrids. *Procedia Engineering* 189: 411-416.

Bauer-Gottwein, P., B.R. Gondwe, G. Charvet, L.E. Marín, M. Rebolloedo-Vieyra, and G. Merediz-Alonso. 2011. Review: The Yucatán Peninsula karst aquifer, México. *Hydrogeol J.* 19: 507-524.

Benmebarek, S., Berrabah, F., Benmebarek, N., Belounar, L. 2015. Effect of Geosynthetic on the Performance of Road Embankment over Sabkha Soils in Algeria: Case Study. *Int. J. of Geosynth. And Ground Eng.* 1:35.

Conrado-Palafox, AL, LN Equihua-Anguiano, M Orozco-Calderón, y E Arreygue-Rocha. 2019. Numerical simulation of karst environments to study subsidence. *Proceedings of the Institution of Civil Engineers - Geotechnical Engineering* 172, nº 4 (2019): 365-376.

Estrada Media, Héctor, and Tuttle. Wes. 2010. Identification of underground karst features using Ground Penetration Radar in Northern Yucatán, México. *Vadose Zone Journal*: 653-661.

Faheem. H., Hassan A.M. 2014. 2D Plaxis Finite Element Modeling of Asphalt-Concrete Pavement Reinforced with Geogrid. *Journal of Engineering Sciences Assiut University Faculty of Engineering*. 42, n° 6: 1336-1348.

Finch, W. 1968. The karst landscape of Yucatan. Washington, D.C.: Distributed by: Clearinhouse, Report Selection aids.

Hussein, M. G., and M. A. Meguid. 2016. A three-dimensional finite element approach for modeling biaxial geogrid with application to geogrid-reinforced soils. *Geotextiles and Geomembranes* 44: 295-307.

Jiand, Y., Nimbalkar, S. 2019. Finite Element Modeling of Ballasted Rail Track Capturing Effect of Geosynthetic inclusions. *Front. Built Environ*. 5, n° 69.

López Ramos, Ernesto. 1975. Geological summary of the Yucatan Peninsula, in Nairn, A.E.M. y colaboradores, eds., The Gulf of Mexico and the Caribbean. New York, Plenum Press, p. 257-282, 1975.

Oh, J. H. 2011. Investigation of Geogrid-Reinforced Flexible Pavement Performance Over Expansive Clay. *Journal of Korean Society of Hazard Mitigations* 11, nº 6: 109-115.

Parry, R H G. 2014. Mohr circles, Stress paths and geotechnics. London: Taylor & Francis Group.

Sheorey, P. 1994. Theory for In-Situ Stress in Isotropic and Transversely Isotropic Rock. *Int. J. Rock Mech. Min. Sci. and Geomech Abstr*. 31(1), 1994: 23-34.

Siriwardane, H., Gonle, R., and Kutuk, B. 2010. Analysis of Flexible Pavements Reinforced with Geogrids. *Geotech. Geol. Eng*. 28: 287-297.

Smart, P. L, P. Beddows, J. Coke, S. Doerr, S. Smith, y F. Whitaker. 2006. Cave development on the Caribbean coast of the Yucatan Peninsula, Quintana Roo, Mexico. *Geological Society of America Special Paper* 404: 105-128.

VDOT. 2013. Geotechnical Design Parameters for Retaining Walls, Sound Barrier Walls and Non-Critical slopes. Virginia Department of Transportation Staunton District.

Xu, Z. H., J. Wu, S. C. Li, B. Zhang, and X. Huang. 2018. Semianalytical solution to determine minimum safety thickness of rock resisting water inrush from filling-type karst caves. *International Journal of Geomechanics* 18, no. 2.